Air Distribution in Rooms, (ROOMVENT 2000)
Editor: H.B. Awbi

NUMERICAL STUDY OF AIRFLOW STRUCTURE OF A CROSS-VENTILATED MODEL BUILDING

T. Kurabuchi[1], M. Ohba[2], A. Arashiguchi[1] and T. Iwabuchi[1]

[1]Department of Architecture, Science University of Tokyo,
Tokyo, 162-0825, JAPAN
[2]Department of Architecture, Tokyo Institute of Polytechnics,
Kanagawa, 243-0297, JAPAN

ABSTRACT

With the purpose of evaluating validity of the application of CFD on the problems of cross-ventilation, numerical simulation was performed, using standard k- ε model and two types of modified k-ε models which improve evaluation accuracy in production term of turbulence energy, and also using LES, and the results were compared with those of the corresponding wind tunnel experiment. As a result, it was found that the defects of the model characteristic to the standard k- ε model could be improved to a certain extent by application of the modified models. However, from the reasons that the effects of improvement are not necessarily remarkable, it was judged that the standard k- ε model could be applicable to a certain extent in case general cross-ventilation phenomenon is to be predicted. On the other hand, when LES is used, the factors such as wind pressure coefficient, turbulence energy, etc. are more accurately reproduced than k- ε type models. Based on these results, the results of calculation of LES were separately assessed, and turbulence structure specific to cross-ventilation was evaluated.

KEYWORDS

Cross-Ventilation, CFD, LES, k-ε model, Wind Tunnel Experiment, Wind Pressure, Natural Ventilation

INTRODUCTION

There are now increasingly strong interests on the utilization of cross-ventilation with the purpose for environmental control in damp heat season and intermediate season. However, there is not much progress in the study to elucidate these problems because cross-ventilation is a complicated turbulence phenomenon where airflow inside and outside a building are interrelated to each other. To overcome the problems, it has been proposed to use numerical simulation, and there have been several cases where the standard k-ε model was actually applied (Frescos, 1998 and Iino et al. 1998). However, it is difficult to apply k- ε model to turbulent flow where turbulence around the flow stagnation point initially plays an important role, and the reliability is not perfectly ensured. Under such circumstances,

we performed calculation using the standard k-ε model and the modified k-ε models to cope with the flow field where flow impingement exists, and also using LES. Based on the comparison with the results of the experiment newly performed, validity of the application of the models was assessed.

OUTLINE OF EXPERIMENT AND NUMERICAL SIMULATION

Building Model and Wind Tunnel Experiment

The study was performed on a building where a pair of openings was mounted at the center of the building as shown in Fig. 1. A model with height of 0.15 m was prepared and wind tunnel experiment was then performed. Fig. 2 shows the profiles of average wind velocity of approach flow and turbulence energy. For the measurement of airflow, split-film type anemometer was used. To determine the ventilation flow rate, a constant quantity of ethylene gas was continuously introduced into inner space of the model, and concentration near the opening on outflow side was measured.

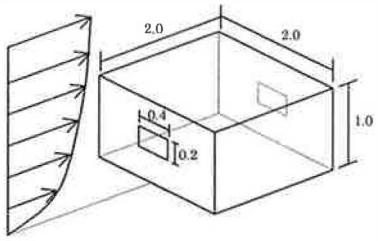

Figure 1 : Flow configuration

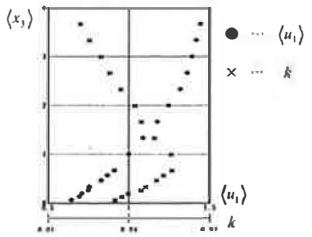

Figure 2 : Profiles of $\langle u_1 \rangle$ and k at inflow boundary

Turbulence Model and Simulation Procedure

It is known that the use of k-ε model often leads to overestimation of the turbulence production term (P_k) because of error in the evaluation of normal stress in case of the flow such as impingement of jet. As shown in Table 1, Launder and Kato (1993) demonstrated that this problem can be improved by evaluating P_k term using a product of characteristic strain parameter S and vorticity parameter ω. However, this modification is disadvantageous in that consistency of energy transfer process between mean flow and turbulent motion may be lost. Murakami et al. (1996) modified eddy viscosity ν_t and proposed a model with consistency and providing similar effects. In this study, three types of k-ε model including the above standard type, LK type and MMK type were assessed. Generalized log-law proposed by Launder and Spalding (1974) was applied for handling wall boundaries. In LES, Smagorinsky model was used with setting constant of the model to 0.13. Wall shear stress was estimated by fitting instantaneous velocity component tangential to wall to the universal wall law. Separate calculation for plane channel flow was performed for generating inflow condition and the stocked data was modified so that distribution of data accurately agrees with the experimental result. After preliminary calculation, formal calculation of 200,000 steps was carried out and analyzed .

TABLE 1

APPLIED k— ε MODELS

Standard k- ε Model	$P_k = \nu_t S^2, \nu_t = C_\mu \frac{k^2}{\varepsilon}$	LK Model	$P_k = \nu_t S\omega, \nu_t = C_\mu \frac{k^2}{\varepsilon}$
$C_\mu = 0.09, S = \sqrt{\frac{1}{2}\left(\frac{\partial\langle u_i\rangle}{\partial x_j} + \frac{\partial\langle u_j\rangle}{\partial x_i}\right)^2}, \omega = \sqrt{\frac{1}{2}\left(\frac{\partial\langle u_i\rangle}{\partial x_j} - \frac{\partial\langle u_j\rangle}{\partial x_i}\right)^2}$		MMK Model	$P_k = \nu_t S^2, \nu_t = C_\mu^* \frac{k^2}{\varepsilon}, C_\mu^* = C_\mu \cdot MIN\left[1.0, \frac{\omega}{S}\right]$

COMPARISONS OF OBSERVED AND SIMULATED RESULTS

Flow Rate

In Table 2, the results of experiment on flow rate are compared with calculations. There was no substantial difference between the models, and all of the results matched well with the experiment.

TABLE 2

COMPARISON OF OBSERVED AND PREDICTED FLOW RATE

experiment	LES	standard	LK	MMK
0.043	0.042	0.041	0.041	0.040

Airflow Patterns of Inside and Outside of the Building

Comparison of the average velocity vector is summarized in Fig. 3. The features of velocity vector in the experimental results were recirculation at the front edge of roof surface (not identified in the experiment due to the limitation on installing probe), extensive recirculation at the lower portion on windward surface, and sudden downfall of the inflow. In the standard k-ε model, the shape of recirculating flow in the lower portion on the windward surface was different, descending of inflow was weak, and that recirculation on the roof surface was not reproduced almost at all. In contrast, in LK model and MMK model, the results were closer to the results of the experiment in the features that descending of inflow is slightly increased, and that the recirculating flow on roof surface is enlarged.

On the other hand, in LES, the recirculation on the lower portion on the windward surface was somewhat longer in the streamwise direction, but, the features such as shape of recirculation, reproduction of recirculation at the front edge of roof, descending of inflow into the building and aspect of wake were very close to the experimental results.

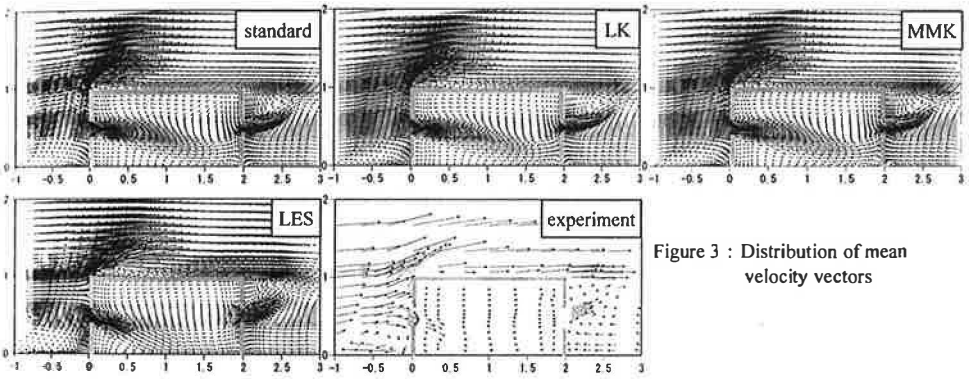

Figure 3 : Distribution of mean velocity vectors

Distribution of Turbulence Kinetic Energy

Fig. 4 shows the comparison of turbulence kinetic energy k. In the experimental results, the value of k reached peak at the front edge of roof surface and there was also a peak in recirculating region on the lower portion on the windward surface. Further, the airflow entering the building reached the maximum value immediately after entering. In the standard k-ε model, the region with high k value is extensively spread from the front edge of roof to the windward surface. In LK model, the level of k value shows extreme decrease on the windward surface of the building Results of MMK model exhibited a distribution intermediate between the standard and LK model. Peak associated with the recirculation on the lower portion on the windward surface was reproduced in none of k-ε models.

On the other hand, in LES, peak values on the lower portion on the windward surface or on the front edge of roof surface were reproduced. Regarding the indoor space of the building, k assumes relatively higher value on the downstream side of the windward opening. In the wake region, the level of k on downstream side of roof surface is somewhat higher than the experiment.

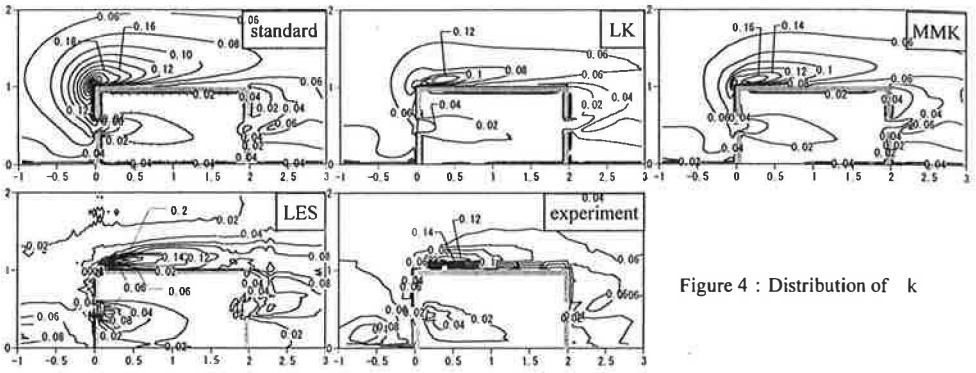

Figure 4 : Distribution of k

Distribution of Wind Pressure Coefficient

Fig. 5 summarizes the comparison between the results of experiment and those of calculation using k-ε models on wind pressure coefficient on external surface of the building in symmetrical surfaces. On the front surface of the building, overestimation of wind pressure coefficient was extremely conspicuous in the standard k-ε model, and the results became closer to the experimental results in the order of LK model and MMK model. On the front edge of the roof surface, recirculation was not sufficiently reproduced in the standard k-ε model, and absolute value of negative pressure on this portion was extremely high. In LK model and MMK model, extreme negative pressure did not occur as the result of the enlargement of recirculation. Magnitude of the calculated ν_t in the vicinity of windward surface is significantly small in the modified models than the standard model, and this would improve accuracy of Reynolds stress, and wind pressure coefficient consequently.

Fig. 6 represents the comparison of calculation results using LES and experiment including the case where openings are not present. There is no sign of overestimation of wind pressure coefficient on the windward surface of the building. In particular, in case there was the opening, wind pressure coefficient was slightly increased on the upper portion of the opening compared with the case of no opening, and the results of the experiment were reproduced very well.

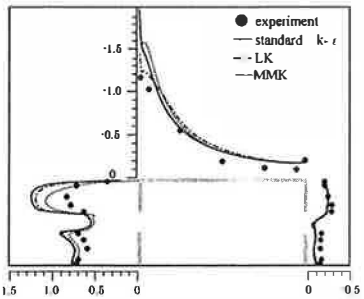

Figure 5 : Distribution of mean pressure coefficient (experiment and k- ε)

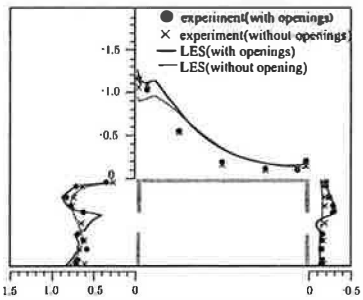

Figure 6 : Distribution of mean pressure coefficient(experiment and LES)

ANALYSIS OF THE RESULT OF LES SIMULATION

As described above, it is evident that the results of LES match far better than k-ε type models with the experimental results, and it can be expected that LES calculation reflects actual conditions even in the case, for which it is difficult to evaluate experimentally. In this respect, we attempted to analyze turbulence structure characteristic in cross-ventilation based on the results of LES calculation.

Momentum Balance near the windward opening

One of the features of the airflow during cross-ventilation is extreme downfall of inflow. To elucidate the cause, we evaluated momentum balance along the central axis, which passes through the center of the opening. The equation of time-averaged velocity component in vertical direction at the plane of symmetry can be approximately expressed as in the equation (1):

$$\frac{\partial\langle\overline{u_3}\rangle}{\partial t} \cong -\frac{\partial\langle\overline{p}\rangle}{\partial x_3} - \frac{\partial\langle\overline{u_1}\rangle\langle\overline{u_3}\rangle}{\partial x_1} - \frac{\partial\langle\overline{u_1'u_3'}\rangle}{\partial x_1} - \frac{\partial\langle\overline{u_3}\rangle\langle\overline{u_3}\rangle}{\partial x_3} - \frac{\partial\langle\overline{u_3'u_3'}\rangle}{\partial x_3} \qquad (1)$$

Fig. 7 shows the average airflow field around the central axis and profile of vertical velocity component (positive in upward direction). Longitudinal profiles of each term in the equation (1) are given in Fig. 8. In the far region from the opening, vertical velocity is turned from positive to negative, and the second term on the RHS of the equation (1) is turned to positive. When the airflow approaches the opening, acceleration occurs and the second term has a high positive value. The cause to deflect the flow downward may be the negative contribution in the equation (1), which offsets the above action. According to Fig. 8, the pressure gradient in the first term of the RHS of the equation (1) opposes from the point -1.5 to around the opening except in the vicinity of opening where only momentum transport by vertical velocity component takes negative value. We may conclude the primary cause of the downfall lies in the pressure gradient due to the recirculation at the lower portion on windward surface.

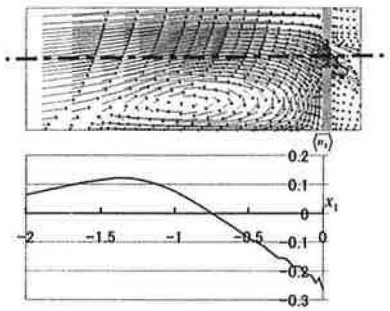

Figure 7 : Flow field near windward opening and longitudinal profile of $\langle\overline{u_3}\rangle$ at central axis of opening

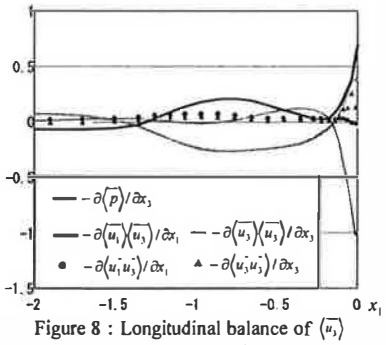

Figure 8 : Longitudinal balance of $\langle\overline{u_3}\rangle$ transport equation at central axis of opening

Deformation of Virtual Flow Tube

To elucidate the mechanism of total pressure loss, the shape of a virtual flow tube passing through the windward opening was calculated by tracing trajectories of passive markers. Fig. 9 shows horizontal and vertical cross sectional views of the flow tube. The flow passing through the opening is turned to a complicated flow where acceleration and deceleration occur within short distance.

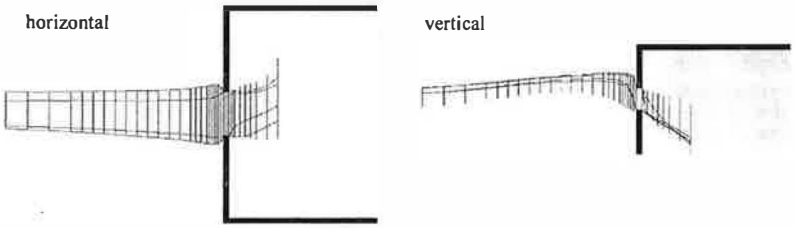

Figure 9 : Cross sectional views of virtual flow tube

Change of Mean Flow Energy

If energy transport equation of mean flow is applied to the flow tube, it is known that the streamwise change of total pressure corresponds to the work on the surface of the flow tube and to the production of k inside the flow tube. Fig. 10 summarizes the changes of static, dynamic and total pressure along the central axis of the opening. The total pressure shows extensive change on upstream side of the opening due to the negligence of streamline direction. The result of integral averaging along the flow tube is shown in Fig. 11. Energy change occurs between static and dynamic pressure due to acceleration and deceleration, but almost no change occurs in total pressure. When reaching the opening, static pressure is decreased at first, and after passing through the opening, dynamic and static pressure are decreased at the same time. The peak of k value is observed immediately after entering the opening, and this is estimated as total pressure loss due to production of k in this region

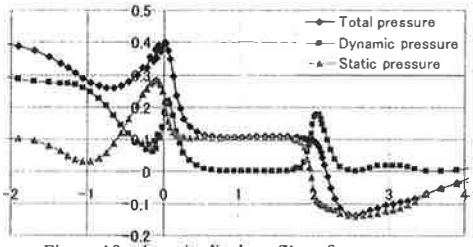

Figure 10 : Longitudinal profiles of pressure at central axis of opening

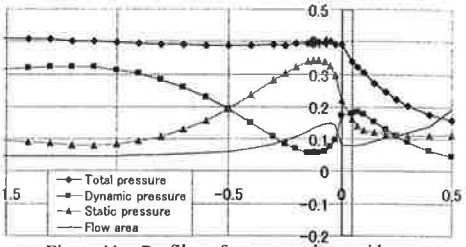

Figure 11 : Profiles of pressure along with the virtual flow tube

CONCLUDING REMARKS

The results of the present study suggest that LK and MMK model slightly improve the problems with the standard k-ε model, however, it is considered that the use of the standard k-ε model can be justified as far as the general cross-ventilation phenomenon is concerned. On the other hand, excellent agreement was observed in the application of LES. Based on these results, the calculation results were analyzed, and it was elucidated that the downfall of the inflow is caused by pressure gradient due to recirculation on the lower portion on the windward surface. Further, based on the results of calculation of a virtual flow tube, the changes along the flow of total pressure loss were evaluated.

Acknowledgement

The authors extend sincere gratitude to TOSTEM Foundation for Construction Materials Industry Promotion for assistance and support to cover research cost of the present study.

Nomenclature

x_i : spatial coordinate (i=1,2,3 : streamwise, spanwise, vertical)
u_i : velocity component
p : pressure
$\langle f \rangle$: time average of f
$\overline{f}$: filtered value of f
$f'' : = \overline{f} - \langle \overline{f} \rangle$
k : turbulent kinetic energy
ε : dissipation rate of k
ν_t : eddy viscosity

References

Freskos G.O. (1998). Influence of Various Factors on the Predistions Furnished by CFD in Cross-Ventilation Simulations, *Proceeding of the 6th International Conference on Air Distribution in Rooms*, **vol.1**, 483-490

Iino Y., Kurabuchi T.,Kobayashi N. and Arashiguchi A. (1998). Study on Airflow Characteristics in and around Building Induced by Cross Ventilation Using Wind Tunnel Experiment and CFD Simulation, *Proceeding of the 6th International Conference on Air Distribution in Rooms*, **vol.2**, 307-314

Launder B.E. and Spalding D.B. (1974). The Numerical Computation of Turbulent Flows, *Comput. Methods APPL. Mech. Eng.*, **3**, 269-289.

Launder B.E. and Kato M. (1993). The Modeling Flow-Induced Oscillations in Turbulent Flow around a Square Cylinder, *ASME Fluid Eng. Conf. Jun.*, **157**, 189-199.

Murakami S., Mochida A., Kondo K., Ishida Y. and Tsuchiya M. (1996). Development of new k-ε model for flow and pressure fields around bluff body, *CWE96*, Colorado, USA.